Indian J. Phys. **71B** (3), 335–347 (1997)

I J P B
- an international journal

Photoabsorption by inner shells in the x-ray range: recent results

Steven T. Manson, Dae-Soung Kim* and Hsiao-Ling Zhou
Department of Physics and Astronomy, Georgia State University
Atlanta, Georgia 30303, USA

Pranawa C. Deshmukh
Department of Physics, Indian Institute of Technology-Madras
Madras, 600 036, INDIA

Zikri Altun
Department of Physics, Marmara University, Istanbul, TURKEY

Abstract: A short review of some recent theoretical work on inner-shell photoabsorption by atoms and ions is presented. The emphasis in this review is on the variety of phenomena exemplified in inner-shell photoabsorption studies, along with how the various methodologies which can be employed focus on different phenomena.

Keywords: photoionization, inner-shell ionization, photodetachment, ions, synchrotron light experiments

PACS numbers: 32.80.Fb, 32.80.Hd, 32.80.Dz

The advent of third generation synchrotron light sources in a number of locations around the world is enabling the study of photoabsorption of atoms

*Present address: Dept. of Physics, Myong-Ji University, Yong-In, Kyungki 449-728, KOREA

with an accuracy and a level of detail previously unobtainable. Furthermore, the new ion rings and other ion sources are extending this advance to ions as well. In a parallel development, the availability of vast amounts of computing power, from supercomputers to workstations, is allowing theory to tackle problems that are increasingly complex employing ever more sophisticated methodologies.

Most of the extant work on photoabsorption deals with the valence electrons of the outer shell. But, owing to the rapidly expanding possibilities of exploring these inner-shell processes experimentally, in this review, a selection of recent theoretical studies of inner-shell photoabsorption are presented in an effort to give the flavor of the new physics that is being learned, the breadth of problems being explored, and the wide variety of theoretical methodologies being utilized. To that end, examples of photabsorption of ground and excited states of neutral atoms are presented, along with examples of photoabsorption by positive and negative ions. In this paper we shall focus only on integrated cross sections; angular distributions have been dealt with elsewhere [1].

Before turning to the presentation of these examples, however, it is useful to briefly point out the basic aspects of the theory of photabsorption. For x-rays of energies below several keV, the dipole approximation is excellent for integrated cross sections [2,3]. Within the framework of the dipole approximation, the cross section for a photoionizing transition from an initial state $|\, i\,\rangle$ to a final state $|\, f\,\rangle$ by x-ray photons of energy $h\nu$, is given by [2]

$$\sigma_{if} = \frac{4\pi^2 \alpha a_0^2}{3 g_i} h\nu |M_{if}|^2 \tag{1}$$

where α is the fine structure constant, a_0 is the Bohr radius, and g_i is the statistical weight (degeneracy) of the initial state. The absolute square of the matrix element is given by [2,3]

$$M_{if}|^2 = \sum_{i,f} \langle f | \sum \vec{r}_j | i \rangle \tag{2}$$

where the sum over j is the sum over the position coordinates of all of the target electrons, and the sums over i and f are sums over the magnetic substates of the initial and final states respectively. The wave functions in Eqs. (1) and (2) are normalized such that

$$\langle i \mid i \rangle = 1 \tag{3}$$

and

$$\langle f \mid f' \rangle = \delta(\varepsilon - \varepsilon'), \tag{4}$$

the usual normalization of continuum wave functions on the energy scale. Note that there are a number of formally equivalent forms of the matrix element, Eq. (2); the one shown is the length form. The other often-used forms are velocity and acceleration [3]. The results of all forms will be the same when exact wave functions are employed. Since we never have exact wave functions, except for the simplest cases, calculation of different forms is often a measure of the quality of the wave functions used. More detail on the theory of photoionization can be found elsewhere [4-8].

As a first example, we consider inner-shell photoionization of the ground state of atomic scandium. This process is of interest because the ground state of Sc, aside from being an open-shell structure, is the first element in the periodic table to have a $3d$ electron bound in the ground state, the first member of the series of $3d$ transition metals. Thus, Sc is a first step in the understanding of the photoabsorption of transition metal atoms and ions. The ground state of Sc is $3s^2\,3p^6\,3d\,4s^2\ ^2D$ outside of a Ne-like core. The calculation was performed using many-body-perturbation theory (MBPT) [9]. All single excitations/ionizations of $4s$, $3d$ and $3p$ electrons were taken into account. This leads to nine possible states of Sc^+: $3s^2\,3p^6\,3d\,4s\ ^{1,3}D$, $3s^2\,3p^6\,4s^2\ ^1S$, $3s^2\,3p^5\,3d\,4s^2\ ^{1,3}P,D,F$. All first order perturbations were taken into account using an integral equation technique [10,11]. In addition, the coupling between the degenerate continuum channels was handled by a diagonalization technique. This is because these degenerate states would require higher order perturbation theory to arrive at a realistic approximation, so diagonalization seemed more reasonable here.

The resulting total photoionization cross section for Sc, in the region of the inner-shell $3p$ thresholds, is shown in Fig. 1 for photon energies between 25 eV and 35 eV and Fig. 2 between 35 eV and 40 eV [12]. In both energy regions, the photoionization is seen to be dominated by autoionizing resonances; the background (non-resonant) cross section is seen to be quite small. The outstanding feature of Fig. 1 is the strength of these autoionizing resonances, resonances which are often small perturbations of the background cross sections. All of these very strong resonances in Fig. 1 have been identified in the calculation to result from $3p \rightarrow 3d$ transitions, i.e., transitions to $3s^2\,3p^5\,3d^2\,4s^2$ autoionizing states. This configuration yields nine multiplets

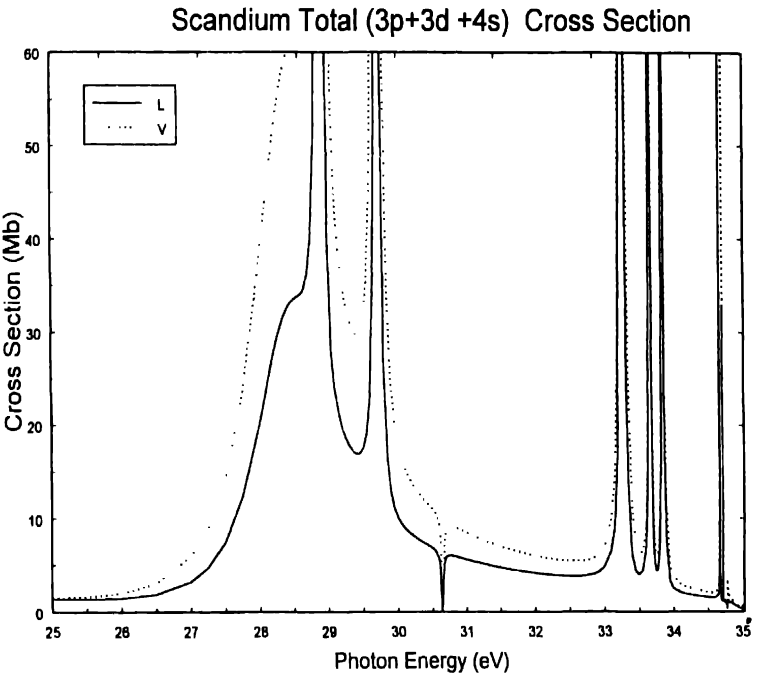

Fig. 1. Total photoionization cross section for Sc in the 25-35 eV photon energy region from Ref. [12]. *L* and *V* refer to length and velocity results, respectively.

optically accessible from the ground state; thus, nine $3p \rightarrow 3d$ resonances are possible. The strength of these resonances is due to the fact that they result from one-electron $\Delta n = 0$ transitions. Since the transition operator is a single-particle operator, it is evident that one-electron transitions will, in general, be much larger than multi-electron transitions. Furthermore, the dipole matrix element, Eq. (2), is largest when the initial and final states overlap very well, i.e., occupy the same region of space. Since the "size" of an atomic wave function is determined by the principal quantum number, n, and very little else, it is clear why the dipole matrix element is largest for $\Delta n = 0$ transitions.

In Fig. 2, the individual resonances are not so strong, in general, but there are many of them and they dominate the spectrum. These resonances are found to be the higher $3p \rightarrow nd$ and $3p \rightarrow ns$ transitions and, although they are not $\Delta n = 0$ transitions, they are one-electron transitions, thus giving them a fair bit of strength. It also seen that there are a number of different series, corresponding to various possible angular momentum couplings, giving rise to

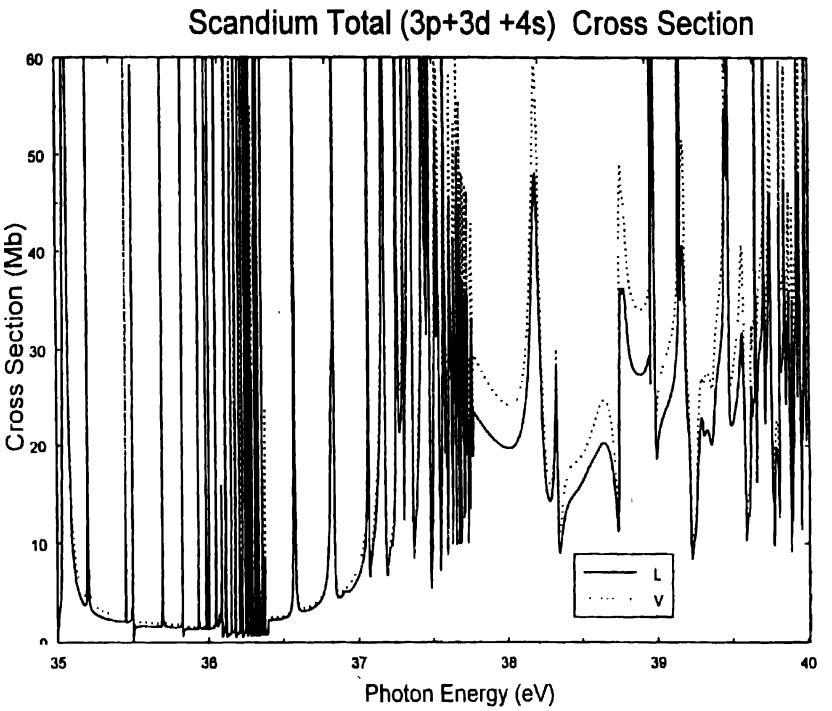

Fig. 2. Total photoionization cross section for Sc in the 35-40 eV photon energy region from Ref. [12]. *L* and *V* refer to length and velocity results respectively.

resonances of varying strength, shape and width.

Finally, note the comparison between the length and velocity results shown in Figs. 1 and 2. Agreement is excellent qualitatively, and generally not bad quantitatively, suggesting that most of the important physics has been included in the calculation.

As a next example, consider the photoionization of the inner shell of an excited atom. For simplicity, we consider is ionization in a low-Z atom, Li, in the $1s^2\,3p$ excited state. This calculation was performed using multiconfiguration Hartree-Fock (MCHF) discrete wave functions [13] and single channel continuum wave functions obtained in the MCHF field [14]. In this methodology, correlation in discrete states, along with the effects of core relaxation, are taken into account rather well, but inter-channel coupling is absent. The results of the calculation [14] are shown in Fig. 3 where the cross sections for leaving the Li^+ ion in $1s\,2p$, $1s\,3p$ and $1s\,4p$ $^{1,3}P$ are shown. The outstanding feature of these results is that the dominant cross section is the $1s^2\,3p \rightarrow 1s\,4p$

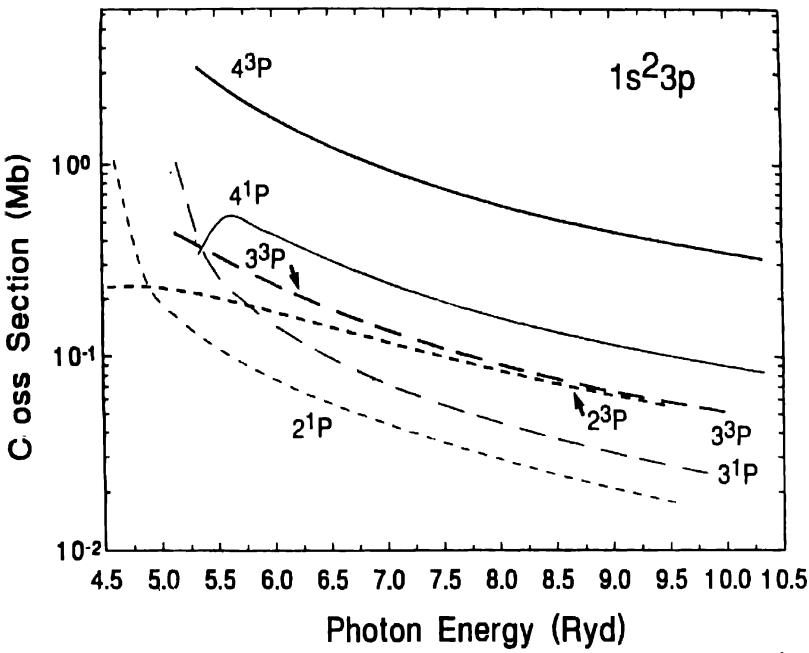

Fig. 3. Photoionization cross sections calculated for $1s$ ionization from the Li $1s^2 3\mathring{p}$ excited state to various $n\,^3P$ and $n\,^1P$ states of the Li^+ ion vs. photon energy from Ref. [14]. The curves are our dipole-length results which are in good agreement with dipole-velocity (not shown).

^3P channel, which represents ionization plus excitation, a two-electron transition. This cross section is seen to dominate over the entire energy range considered. In addition, the next-largest cross section is the $1s^2 3p \rightarrow 1s4p\ ^1P$ channel, again ionization plus excitation.

In order to understand why these two-electron transitions are significantly larger than the one-electron transitions, it necessary to scrutinize the dominant term in the transition matrix element, which, apart from angular factors, is given by

$$M_{np}(^{1,3}P) = A(^{1,3}P)\langle\, 1s_i \mid 1s_f\rangle\langle\, 3p_i \mid np_f\rangle\langle\, 1s_i \mid r \mid \varepsilon p_f\rangle \qquad (5)$$

for a $1s_i^2 3p_i \rightarrow 1s_f\, np_f\, \varepsilon p$ transition, where $A(^{1,3}P)$ is the angular factor. To begin with, $A(^3P) = -3\, A(^1P)$ so that, all other things being equal, the triplet cross sections would be a factor of three larger than the corresponding singlet cross sections, thus explaining the singlet-triplet magnitude difference seen in

Fig. 3.

More importantly, however, the only significant change in the dominant term in the matrix element with changing n of the np_f electron, comes from the overlap term in Eq. (5), $\langle\, 3p_i \mid np_f \,\rangle$; the cross section is proportional to the square of this overlap term. Calculations [14] show that for the ^3P final states, the squares of this overlap factor are 0.089, 0.107, and 0.759 for $2p$, $3p$, and $4p$ final states respectively, while for the ^1P cases, the results are 0.090, 0.162, and 0.718, respectively. The fact that the $\langle\, 3p_i \mid 4p_f \,\rangle$ overlaps are by far the largest means that the cross section for $1s\,4p$ final states are the largest, thus explaining the higher energy results shown in Fig. 3.

To understand why the overlaps favor the $3p \rightarrow 4p$ so strongly, note that a reasonably highly excited state of Li is virtually completely screened by the $1s^2$ core. Thus, the excited electron "sees" a charge of unity. Similarly, in the Li^+ ion, the excited electron "sees" a charge of two, so that the $3p_i$ of the final state is considerably more compact than the $3p_i$ of the initial state. Thus, the principal overlap of the $3p_i$ wave function is with $4p_f$ which, owing to the increased charge it "sees", occupies the same region of space as the $3p_i$. The effect is quite dramatic when the initial state excited electron "sees" a charge of one and the final state excited electron "sees" a charge of two, so that the effective charge changes by a factor of two. For lower excited states, or the ground state, where the wave function of the outermost shell penetrates the core, the removal of an inner-shell electron still changes the effective charge by one, but the change is nowhere near a factor of two. This is why this effect does not generally occur for ground or lowly excited states. These conclusions have recently been confirmed by R-matrix calculations as well [15].

From the above discussion, it is clear that this effect is not peculiar to excited p-states; it will be in evidence for any angular momentum. It is also clear that these two-electron transitions will dominate the photoionization in inner-shell photoionization of excited states of atoms throughout the periodic spectrum.

Another example of inner-shell photoabsorption concerns the $1s$ photodetachment of the metastable $1s\,2s\,2p\,^4P$ state of He^-; the $j = 5/2$ component has a lifetime of about 1 ms. This is the lowest bound state of He^-. The calculated total photodetachment cross section of He^- in the vicinity of the $1s$ detachment threshold [16], using the MCHF methodology, is given in Fig. 4. From this figure it is seen that in the 35-50 eV photon energy region, the photodetachment cross section is dominated by three structures; a huge resonance at about 38 eV, a large spike just above the $1s$ detachment threshold, and a gentler and broader maximum with a threshold several eV above the $1s$ detachment threshold.

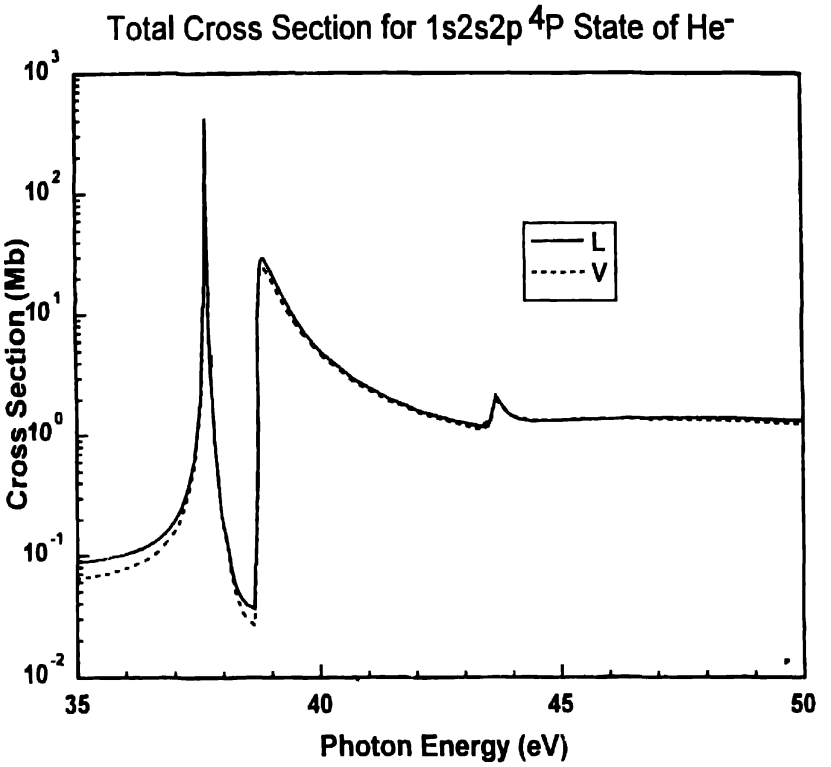

Fig. 4. Total photodetachment cross section for the $1s2s2p\ ^4P$ state of He^- in the vicinity of the $1s$ detachment threshold from Ref. [16]. The solid curve is the length result and the dashed line is velocity.

The resonance in the 38 eV region occurs in the $\{1s2p\ ^3P\}\ np\ ^4P$ channel and is, basically, a $2s2p^2\ ^4P$ resonance which lies just below the opening of the $1s$ detachment channel; the $\{1s2p\ ^3P\}\ np\ ^4S,^4D$ channels do not have any significant effect in this region. This resonance is an example of a hollow negative ion state since it contains all $n = 2$ electrons with an empty n=1 shell; these states in neutral atoms, particularly Li, have been the subject of much recent scrutiny [17]. In the photoionization of ground state neutral atoms, however, they tend to be small blips on a large non-resonant background [17]. The $2s2p^2$ resonance in He^-, on the other hand, dominates the photodetachment cross section, as seen in Fig. 4. The reason for this difference is that the $1s2s2p \rightarrow 2s2p^2$ transition in He^- is a one-electron transition and, thereby, quite strong. In studies of the photoionization of ground-state atoms, on the other hand, these hollow states can be reached only by two-electron transi-

tions.

The roughly 30 Mb spike just a few meV above the 1*s* detachment threshold is the 1*s* non-resonant photodetachment cross section. Since photodetachment cross sections must be zero at threshold [18], a maximum above threshold is inevitable. But, although the 1*s* orbital in this He^- state is virtually unscreened and quite similar to the 1*s* of He^+, there are two major differences in the cross sections; the final continuum states are dramatically different in the two cases, particularly near threshold, and the effects of correlation, as manifested by multiconfiguration wave functions, which give importance to a number of terms in the dipole matrix element for He^-. These two differences lead to a maximum in the 1*s* photodetachment cross section of about 30 Mb, much larger than is ever seen for 1*s* photoionization of atoms, along with a much more rapid fall-off with energy, as compared to neutral atoms.

Starting at about 45 eV, the total cross section is dominated by a much gentler maximum, as seen in Fig. 4 . This is due to 1*s* photodetachment plus excitation of the residual He atom to the next excited ^3P states. These next excited states cannot be adequately described by a single configuration; they are roughly 50-50 admixtures of $2s\,3p$ and $2p\,3s$. Contrary to what occurs in He photoionization [19] both the state designated "+" and the one called "-" have appreciable oscillator strength, the initial sharper maximum is due to the "-" state, while the following broader maximum results from the "+" state. Owing to the rapid falloff of the main 1*s* detachment cross section, discussed above, along with the relaxation effects which occur in connection with inner-shell ionization of excited states, as soon as this cross section reaches its maximum, it dominates the cross section. Furthermore, the shape of this cross section is dramatically different from the shape of the main 1*s* cross section, indicating that the relationship between them is not a simple shake-off effect, but rather a complex function of the details of correlation. The calculations suggest that the dominance of the detachment plus excitation channel persists to higher energy as well.

As a final example, work on the photoionization of positive ions of the Mg isoelectronic sequence, using the relativistic-random-phase approximation (RRPA) [20,21] as an adjunct to multi-channel quantum defect theory (MQDT) [19] is presented. The photoionization cross- section of the 3*s* shell of magnesium-like Al^+, below the $2p_{3/2}$ threshold [22], is shown in Fig.5, where resonances belonging to both $2p_{3/2}$ and $2p_{1/2}$ Rydberg series are seen; in the region of $h\nu = 3.506$ au the $2p_{3/2} \rightarrow 16s$, $15d$ resonances are seen to be in close proximity with the $2p_{1/2} \rightarrow 10s$, $9d_{3/2}$. Despite this proximity, however, the $2p_{3/2}$ resonances in this range remain substantially in the same repetitive pattern as the $2p_{3/2}$ resonances at higher and lower energy, as seen in Fig. 5. In other words, the $2p_{1/2}$ resonances appear to leave the $2p_{3/2}$ res-

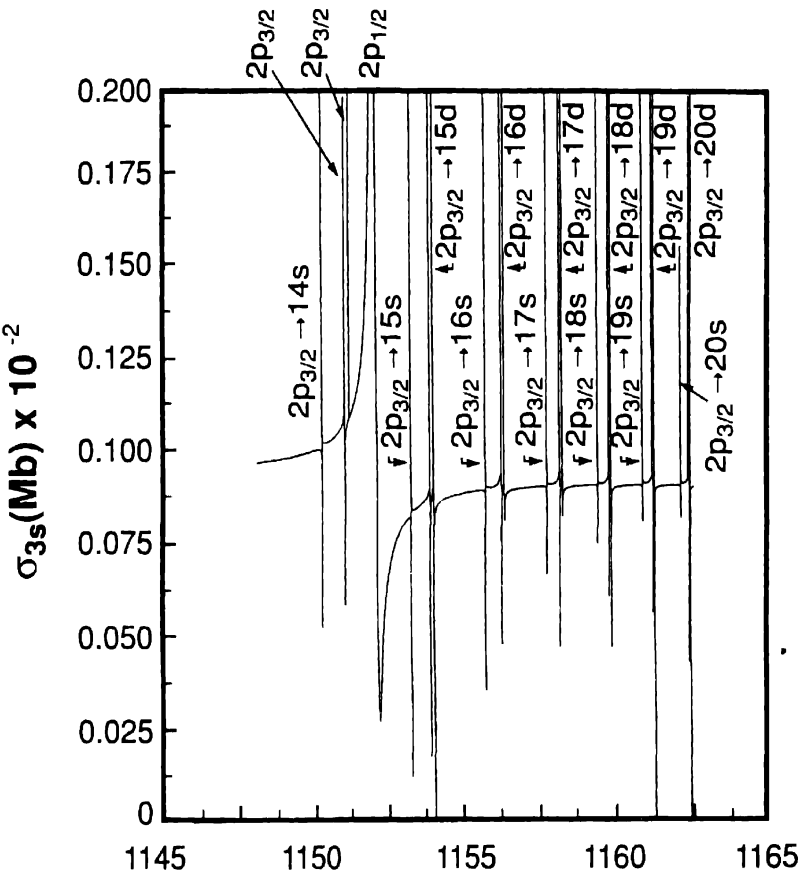

Fig. 5. Photoionization cross section of the 3*s* shell of Mg-like Al^+ below the 2*p* thresholds from Ref. [22]. The character of the resonances are labelled. The lowest $d_{3/2}$ and $d_{5/2}$ resonances shown are labelled independently; the higher d resonances follow the same pattern but, for clarity they are not labelled individually.

onances largely unchanged in Al^+. The presence of the $2p_{1/2}$ resonances, then, leaves the $2p_{3/2}$ resonances looking rather like the case of neutral Mg [23]. At this point it is useful to note that when resonances converging to differing thresholds are present, as has been seen for Al^+, the spectrum becomes extremely difficult to interpret. This can be achieved, however, by decoupling the $2p_{3/2}$ and $2p_{1/2}$ channels from each other, i.e., by doing the calculation with only the 3*s* and $2p_{3/2}$ channels or the 3*s* and $2p_{1/2}$ channels. Comparing the two, it is a simple matter to distinguish between $2p_{3/2}$ and $2p_{1/2}$ resonances. This technique was used throughout this work.

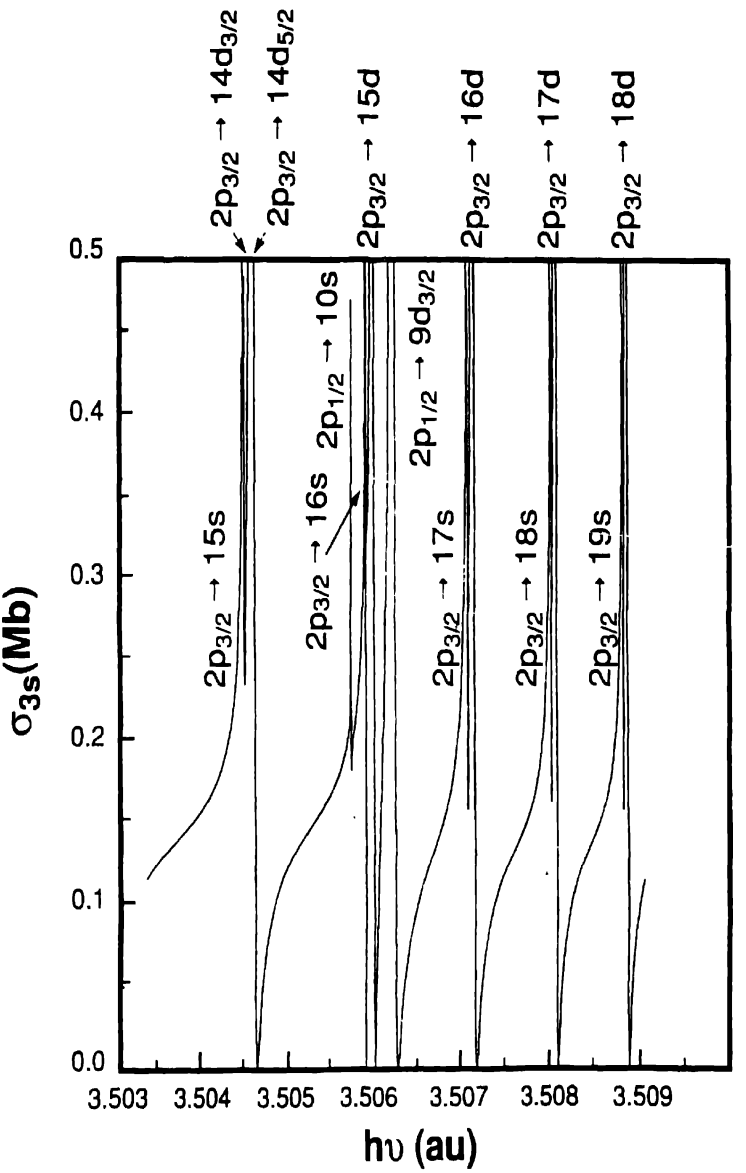

Fig. 6. Photoionization cross section of the 3*s* shell of Mg-like Lr^{91+} below the 2*p* thresholds from Ref. [22]. The character of the resonances are labelled. The lowest $d_{3/2}$ and $d_{5/2}$ resonances shown are labelled independently; the higher *d* resonances follow the same pattern but, for clarity they are labelled individually.

The autoionization resonances in the $3s$ photoionization cross-section of Lr^{91+}, the highest Z considered, are shown in Fig. 6. To our knowledge, it is for the first time that the stability of the ab-initio MQDT parameters has been found over such a wide range of energies; this enabled the calculation of the resonances shown in Fig.4. In Lr^{91+} we see that the resonances $2p_{3/2} \rightarrow 15d$-$20d$ have similar shapes whereas the profiles of $2p_{3/2} \rightarrow 14d_{3/2}$, $14d_{5/2}$ are considerably different. This can be attributed to the effect of series perturbation due to $2p_{1/2} \rightarrow 4d_{3/2}$ resonance which alters the profile of the neighboring resonances significantly and also affects the background cross-section in the region. Thus, in Lr^{91+} the $2p_{1/2}$ resonance is seen to have a pronounced affect on the $2p_{3/2}$ resonances. This is clearly indicates that the $2p_{1/2}$ resonances increase in strength relative to the $2p_{3/2}$ along the isoelectronic sequence. The $2p_{1/2} \rightarrow 4d_{3/2}$ resonance dominates the Lr^{91+} spectrum over an energy range of 3 au (80 eV), as seen in Fig 6. The series perturbation that had minimal effect in Al^+ is now a dominant feature of the spectrum.

Acknowledgements

This work was supported by the National Science Foundation and the National Aeronautics and Space Administration.

References

[1] S. T. Manson, J. Electron Spectrosc. **66**, 117 (1993).

[2] D. R. Bates, Mon. Not. Roy. Astron. Soc. **106**, 432 (1946).

[3] H. A. Bethe and E. E. Salpeter, *Quantum Mechanica of One- and Two-Electron Atoms* (Springer, Berlin, 1957), pp. 247-323.

[4] U. Fano and J. W. Cooper, Rev. Mod. Phys. **40**, 441 (1968).

[5] S. T. Manson, Adv. Electonics Electron Phys. **41**, 73 (1976).

[6] S. T. Manson and D. Dill, in *Electron Spectroscopy*, Vol. 2, edited by C. R. Brundle and A. D. Baker (Academic Press, New York, 1978), pp. 157-195.

[7] A. F. Starace, in *Handbuch der Physik*, Vol. 31 edited by W. Mehlhorn (Springer, Berlin, 1982), pp. 1-121.

[8] M. Ya. Amusia, *Atomic Photoeffect* (Plenum Press, New York, 1990).

[9] H. P. Kelly, in *Photoionization and Other Probes of Many-Electron Interactions*, edited by F.Wuilleumier, (Plenum Press, New York, 1976), pp. 83-109.

[10] Z. Altun, J. Phys. B **25**, 2279 (1992).

[11] J. J. Boyle, Z. Altun and H. P. Kelly, Phys. Rev. A **47**, 4811 (1993).

[12] Z. Altun and S. T. Manson, Europhys. Lett. **33**, 17 (1996).

[13] C. F. Fischer, Comput. Phys. Commun. **64**, 369 (1991).

[14] Z. Felfli and S. T. Manson, Phys. Rev. Lett. **68**, 1687 (1992).

[15] J. C. Chang, Vo Ky Lan, P. Faucher and F. Bely-Dubau, in *XIX ICPEAC: Scientific Program and Abstracts of Contributed Papers*, edited by J. B. A. Mitchell, J. W. McConkey and C. E. Brion (ICPEAC, Whistler, B. C., Canada, 1995), p. 317.

[16] D. S. Kim, H.-L. Zhou and S. T. Manson, Phys. Rev. Lett. (submitted).

[17] L. M. Kiernan, E. T. Kennedy, J.-P. Mosnier, J. T. Costello and B. F. Sonntag, Phys. Rev. Lett. **72**, 2359 (1994).

[18] S. J. Buckman and C. W, Clark, Rev. Mod. Phys. **66**, 539 (1994), and references therein.

[19] U. Fano, Rept. Prog. Phys. **46**, 97 (1983), and references therein.

[20] W. R. Johnson, C. D. Lin, K. T. Cheng and C. M. Lee, Physica Scripta **21**, 409 (1980).

[21] W. R. Johnson and K. T. Cheng, Phys. Rev. A **20**, 978 (1979).

[22] G. N. Haque, P. C. Deshmukh and S. T. Manson, Phys. Rev. A (submited).

[23] P. C. Deshmukh and S. T. Manson, Phys. Rev. A **28**, 209 (1983).